

## Halo-independent tests of dark matter direct detection signals

---

**Juan Herrero-Garcia\***

*Department of Theoretical Physics, Royal Institute of Stockholm (KTH)*

*E-mail: [juhg@kth.se](mailto:juhg@kth.se)*

We discuss a new halo-independent framework that can be used to relate dark matter direct detection signals with constraints from LHC, indirect detection and the thermal freeze-out paradigm. From an observed direct detection signal we show that a lower bound on the product of the dark matter-nucleon cross section and the energy density, that is independent of the velocity distribution, can be derived. This allows to obtain strong and robust halo-independent constraints on particle physics models. We also extend this framework to the case of annual modulation signals and we illustrate the use of the lower bounds with the DAMA signal.

*The European Physical Society Conference on High Energy Physics  
22–29 July 2015  
Vienna, Austria*

---

\*Speaker.

## 1. Motivation: halo-independent comparisons of direct detection signals

It is well-known that dark matter (DM) direct detection (DD) signals are very sensitive to the astrophysical uncertainties of the halo, which makes their interpretation with other results astrophysics-dependent. For instance, typically a Maxwellian distribution of velocities truncated at the galactic escape velocity (the Standard Halo Model (SHM)), is assumed, while  $N$ -body simulations indicate a more complicated DM halo. In this talk we develop a new framework that allows one to compare DD signals with other limits from colliders, indirect detection or the relic abundance independently of the velocity distribution  $f(v)$ .

Let us first review the basic expressions of DM DD and the well-known HI framework used for comparing among DD signals. For SI elastic interactions, the DM event rate in underground detectors can be written as

$$\mathcal{R}(E_R, t) = A^2 F_A^2(E_R) \tilde{\eta}(v_m, t), \quad \text{with} \quad \tilde{\eta}(v_m, t) \equiv \mathcal{C} \int_{v_m}^{\infty} dv v \tilde{f}_{\text{det}}(v, t), \quad (1.1)$$

where  $F_A(E_R)$  is a nuclear form factor and

$$\tilde{f}_{\text{det}}(v) \equiv \int d\Omega f_{\text{det}}(v, \Omega), \quad \mathcal{C} \equiv \frac{\rho_\chi \sigma_{\text{SI}}}{2m_\chi \mu_{\chi p}^2}, \quad v_m = \sqrt{\frac{m_A E_R}{2\mu_{\chi A}^2}}. \quad (1.2)$$

Here  $\sigma_{\text{SI}}$  is the total DM–proton scattering cross section at zero momentum transfer,  $\mu_{\chi p}$  is the DM–proton reduced mass and  $\rho_\chi$  is the local DM mass density.  $f_{\text{det}}(v)$  is the unknown velocity distribution in the detector rest-frame.

For fixed  $m_\chi$ , one can translate  $E_R$  into  $v_m$  by using eq. (1.2), and then  $\tilde{\eta}(v_m, t)$  has to be the same for any experiment [1]. This is the basis of the HI framework developed to compare DD signals and limits. Recently in ref. [2] it was extended in order to compare a DD signal with the neutrino flux from DM annihilations in the Sun.

## 2. A new HI framework to compare direct detection signals with local density measurements, the LHC, the relic abundance and indirect detection limits

In the following we further extend the HI frameworks discussed in the previous section by deriving a bound that allows to compare the DD signals with limits from the LHC, the relic abundance and indirect detection, and we do this both for constant rates and for annual modulations.

### 2.1 A bound on the halo integral

Using the definition of  $\bar{\eta}(v_m)$  and the normalization of  $f_{\text{det}}(v)$  we can obtain [3, 4, 5]:

$$1 \equiv \int_0^\infty d^3v f_{\text{det}}(\vec{v}) \equiv \int_0^\infty \bar{\eta}(v) dv \quad (2.1)$$

$$\geq \bar{\eta}(v_1) v_1 + \int_{v_1}^{v_2} dv \bar{\eta}(v) \quad (2.2)$$

$$\geq \bar{\eta}(v_1) v_1, \quad (2.3)$$

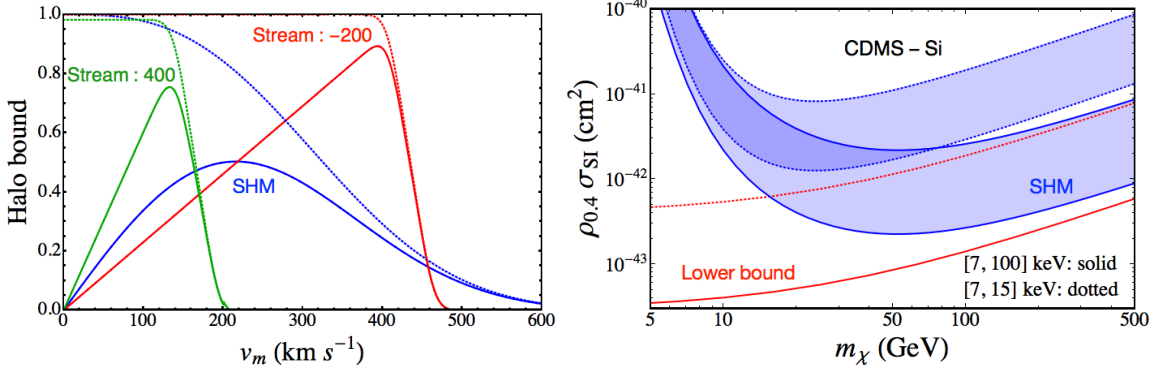


**Figure 1:** Left: The solid (dotted) curves show the rhs of eq. (2.3) (eq. (2.2)) for the SHM (blue) and for two stream examples (red, green) aligned with the Sun, with velocities  $-200$  (red) and  $+400$  km/s (green) relative to the galaxy. Right: CDMS-Si 90% CL lower bound (SHM interval) in red (blue) on  $\rho_{0.4} \sigma_{\text{SI}}$  ( $\rho_{0.4} \equiv \rho_{\chi}/(0.4 \text{ GeV cm}^{-3})$ ) versus  $m_{\chi}$ , for energy ranges  $[7, 15]$  keV (dotted) and  $[7, 100]$  keV (solid).

where from the first to the second line we used that below the threshold  $v_1$  the minimum is obtained for constant  $\bar{\eta}(v) = \bar{\eta}(v_1)$ , as it is a monotonously decreasing function, and in the last line we dropped the second term.

In the left panel of fig. 1 we show with solid curves the product  $v_m \eta(v_m)$ , i.e., the rhs of eq. (2.3), for the SHM as well as for two cold DM streams. We also show with dotted curves the rhs of eq. (2.2) with  $v_1 = v_m$  and  $v_2 \rightarrow \infty$ . If they are  $\sim 1$ , the inequality is saturated, while for  $\ll 1$  they are weak. For the SHM one can see that the lower bound of eq. (2.3) is reasonably strong for  $50 \lesssim v_m \lesssim 400 \text{ km s}^{-1}$ . For high velocities, both are similar, whereas for low velocities eq. (2.2) is close to saturated and provides stronger bounds than eq. (2.3).

## 2.2 Constant rates

From the expressions of the previous section we can derive two HI lower bounds on  $\rho_{\chi} \sigma_{\text{SI/SD}}$  [5]:

1. Using eq. (2.3), we obtain a bound that is applicable when only some number of signal events has been measured, i.e., when a DM has produced a “bunch of events” [5]:

$$\rho_{\chi} \sigma_{\text{SI}} \geq \frac{2m_{\chi} \mu_p^2}{MT \langle 1/v_m^A \rangle_{E_1}^{E_2}} N_{[E_1, E_2]} \quad \text{“Events bound”}. \quad (2.4)$$

In the right panel of fig. 2 we apply it to the CDMS-Si signal [6]. Astrophysical measurements imply that  $\rho_{\chi} \lesssim 0.6 \text{ GeV cm}^{-3}$ , and thus  $\sigma_{\text{SI}} \lesssim 3 \cdot 10^{-43} \text{ cm}^2$  are disfavoured.

2. Using eq. (2.2), we get a bound applicable when the spectrum is measured [5] (see also ref. [7]):

$$\rho_{\chi} \sigma_{\text{SI}} \geq \frac{2m_{\chi} \mu_{\chi p}^2}{A^2} \left( v_1 \frac{\mathcal{R}(E_1)}{F_A^2(E_1)} + \int_{v_1}^{v_2} dv \frac{\mathcal{R}(E_R)}{F_A^2(E_R)} \right) \quad \text{“Spectrum bound”}. \quad (2.5)$$

In the left panel of fig. 2 we illustrate its use with Xe mock data. In order to compare with LHC upper limits we use a simplified model with a DM Majorana fermion  $\chi$ , that has axial-vector couplings (SD) of equal magnitude to  $u, d, s, c$  mediated by a  $Z'$ . We use 95% CL CMS 8 TeV limits on monojets [8] based on  $19.7 \text{ fb}^{-1}$ .

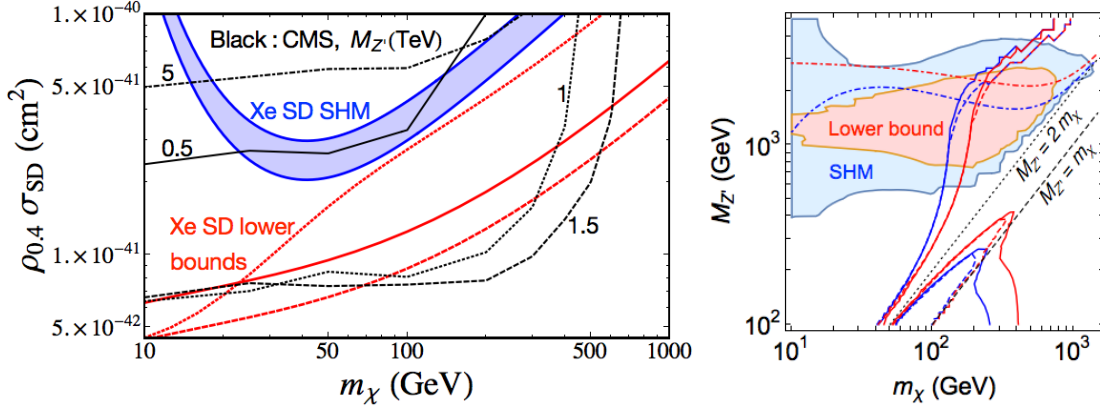


**Figure 2:** Left: The red solid, dotted and dashed curves correspond to the bounds from eq. (2.4), eq. (2.5), and just the first term of eq. (2.5), respectively, for Xe mock data, while the blue-shaded region corresponds to the SHM. Black curves show CMS 95% CL upper limits for the simplified model for various  $M_{Z'}$  (in TeV). Right: The colored regions in the  $m_\chi - M_{Z'}$  plane (blue for SHM, red for lower bound) are excluded by LHC. To the right of the solid (with  $g_\chi = g_q$ ) and dashed (with  $g_\chi = 10g_q$ ) curves the DM cannot be a thermal relic, and above the dotted-dashed curves the DD signal implies  $\Gamma_{Z'} > M_{Z'}/2$ .

In the right panel of fig. 2 we show the parameter space in the  $m_\chi - M_{Z'}$  plane that is excluded as an explanation of the assumed DD signal in Xe, both for the SHM (blue) and with our  $f(v)$ -independent bounds (red). The lower bound on the DD cross section implies a lower bound on the annihilation cross section, and therefore an upper bound on the relic abundance. We also show the constraint  $\Omega_{\text{bound}/\text{SHM}} < \Omega_{\text{obs}}$ , and thus, in the region to the right of these lines the DM providing the DD signal cannot be produced thermally. Moreover, the bound on  $\Omega$  is also valid for multi-component DM if the DD signal is given by one species and  $\rho_\chi \propto \Omega_\chi$ , which is the case for cold DM. Furthermore it is conservative in the sense that more channels can only make it stronger.

The same procedure can be done for different DM particle physics models, and also comparing with indirect detection limits in those cases where there is non-negligible annihilation cross-section (unlike the simplified model presented here, where  $\sigma_{\text{ann}}$  is p-wave suppressed).

### 2.3 Annual modulations

DM gives rise to annual modulation signals in DD experiments [9, 10]. In this case one can also obtain lower bounds on  $\rho_\chi \sigma_{\text{SI}/\text{SD}}$  [11]. By doing an expansion on the Earth’s velocity ( $v_e(t)$ ) and some mild assumptions about the halo one can derive the following upper bounds on the modulation amplitude  $A_\eta(v)$  (the time-dependent part of  $\tilde{\eta}(v_m, t)$ , see eq. (1.1)) [12, 13, 14]:

$$\int_{v_1}^{v_2} dv A_\eta(v) \leq v_e \left( \bar{\eta}(v_1) + \int_{v_1}^{v_2} dv \frac{\bar{\eta}(v)}{v} \right) \quad \text{“General halo”,} \quad (2.6)$$

$$\int_{v_1}^{v_2} dv A_\eta(v) \leq \sin \alpha v_e \bar{\eta}(v_1) \quad \text{“Symmetric halo”.} \quad (2.7)$$

For the “General halo” the bound is independent of the phase, which is free. However, for the “Symmetric halo” the phase is independent of  $v_m$  (and therefore independent of  $E_R$ ), and fixed. The SHM is included in this last case, with  $\sin \alpha \simeq 0.5$  and the phase being equal to June 2nd.

By applying eq. (2.2) in the “General halo”, eq. (2.6), (and in the “Symmetric halo”, eq. (2.7)), we can derive lower bounds on  $\rho_\chi \sigma_{\text{SI/SD}}$ , which do not depend on  $f(v)$  [11], for general haloes:

$$\rho_\chi \sigma_{\text{SI}} \geq \frac{2m_\chi \mu_p^2}{A^2} \frac{1}{v_e} \left( \frac{2}{v_1} - \frac{1}{v_2} \right)^{-1} \int_{v_1}^{v_2} dv \frac{\mathcal{M}(v)}{F_A^2(E_R)} \quad \text{“General bound”}, \quad (2.8)$$

and for symmetric ones:

$$\rho_\chi \sigma_{\text{SI}} \geq \frac{2m_\chi \mu_p^2}{A^2} \left( \frac{1}{v_1} \right)^{-1} \frac{1}{\sin \alpha v_e} \int_{v_1}^{v_2} dv \frac{\mathcal{M}(v)}{F_A^2(E_R)} \quad \text{“Symmetric bound”}. \quad (2.9)$$

If a DD experiment observes an annual modulation, eq. (2.8) (“General bound”) and eq. (2.9) (“Symmetric bound”) provide lower bounds on the product  $\rho_\chi \sigma_{\text{SI}}$  which are independent of  $f(v)$ . Notice that one can also use those of eq. (2.4) (“Events bound”) and eq. (2.5) (“Spectrum bound”) using that modulations should be smaller than rates ( $A_\eta \leq \bar{\eta}$ ). However, the ones based on an expansion on  $v_e$ , eqs. (2.8) and (2.9), are stronger by a factor  $\sim v/v_e$  (with  $v > v_m(E_{\text{th}})$ ).

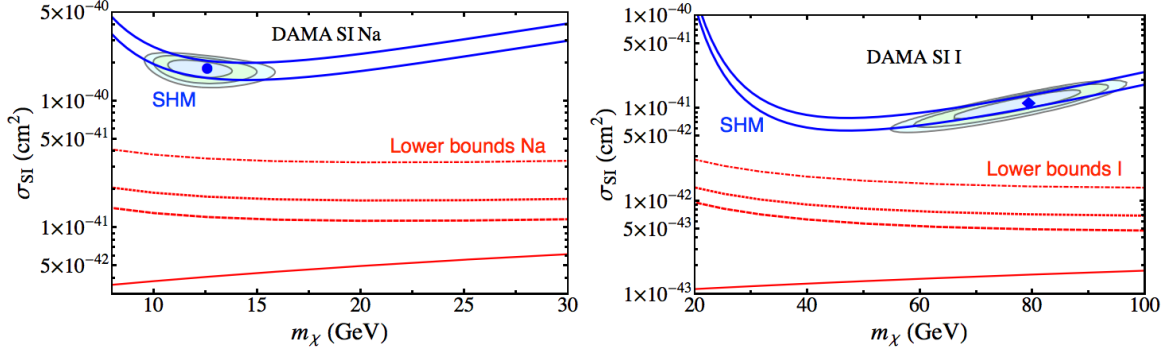


**Figure 3:** DAMA results for SI interactions on Na (left) and I (right). The SHM allowed parameter space at the 90% CL is encoded between the solid blue lines. The 90% CL lower bounds are shown in red from bottom to top: the “Spectrum bound” of eq. (2.5) (solid red), the “General bound” of eq. (2.8) (dashed red) and the “Symmetric bound” of eq. (2.9) (dotted red for  $\sin \alpha = 1$ , dotted-dashed red for  $\sin \alpha = 0.5$ ). The SHM  $\Delta\chi^2 = 2.3, 5.99, 9.21$  contours (CL of 68.27, 95, 99%) are shown in blue, green and light blue, respectively, together with the best-fit points (blue marks).

In fig. 3 we illustrate the bounds for DAMA’s annual modulation [15]. We show the 90% CL lower bounds on the SI cross section (red), together with the SHM preferred regions (blue), for  $\rho_\chi = 0.4 \text{ GeV cm}^{-3}$ . By using that from astrophysical measurements  $\rho_\chi \lesssim 0.6 \text{ GeV cm}^{-3}$ , we obtain for the very conservative “General bound” (dashed red) that  $\sigma_{\text{SI}} \lesssim 8 \cdot 10^{-42} (3 \cdot 10^{-43}) \text{ cm}^2$  are disfavoured for  $m_\chi = 12 \text{ GeV}$ , scattering on Na ( $m_\chi = 79 \text{ GeV}$ , scattering on I). For SD  $\sigma_{\text{SD}} \lesssim 3 \cdot 10^{-38} (2 \times 10^{-38}) \text{ cm}^2$ , for  $m_\chi = 12 \text{ GeV}$ , scattering on Na ( $m_\chi = 63 \text{ GeV}$ , scattering on I). Compared to the SHM, the bounds are roughly between  $\sim 0.5 - 1.5$  orders of magnitude weaker, but of course with the advantage of being completely independent of  $f(v)$ .

In order to be as conservative as possible it would be desirable that, when a positive DD signal is observed, in addition to the typical SHM preferred regions, the community also shows the results using the  $f(v)$ -independent lower bounds here discussed and derived in refs. [5, 11], in a similar way as shown in fig. 3 for the DAMA signal.

## References

- [1] P. J. Fox, J. Liu, and N. Weiner, *Integrating Out Astrophysical Uncertainties*, *Phys. Rev.* **D83** (2011) 103514, [[arXiv:1011.1915](#)].
- [2] M. Blennow, J. Herrero-Garcia, and T. Schwetz, *A halo-independent lower bound on the dark matter capture rate in the Sun from a direct detection signal*, *JCAP* **1505** (2015), no. 05 036, [[arXiv:1502.03342](#)].
- [3] B. J. Kavanagh and A. M. Green, *Improved determination of the WIMP mass from direct detection data*, *Phys. Rev.* **D86** (2012) 065027, [[arXiv:1207.2039](#)].
- [4] B. Feldstein and F. Kahlhoefer, *Quantifying (dis)agreement between direct detection experiments in a halo-independent way*, *JCAP* **1412** (2014), no. 12 052, [[arXiv:1409.5446](#)].
- [5] M. Blennow, J. Herrero-Garcia, T. Schwetz, and S. Vogl, *Halo-independent tests of dark matter direct detection signals: local DM density, LHC, and thermal freeze-out*, *JCAP* **1508** (2015), no. 08 039, [[arXiv:1505.05710](#)].
- [6] **CDMS** Collaboration, R. Agnese et al., *Silicon Detector Dark Matter Results from the Final Exposure of CDMS II*, *Phys. Rev. Lett.* **111** (2013), no. 25 251301, [[arXiv:1304.4279](#)].
- [7] F. Ferrer, A. Ibarra, and S. Wild, *A novel approach to derive halo-independent limits on dark matter properties*, *JCAP* **1509** (2015), no. 09 052, [[arXiv:1506.03386](#)].
- [8] **CMS** Collaboration, V. Khachatryan et al., *Search for dark matter, extra dimensions, and unparticles in monojet events in proton–proton collisions at  $\sqrt{s} = 8$  TeV*, *Eur. Phys. J.* **C75** (2015), no. 5 235, [[arXiv:1408.3583](#)].
- [9] A. K. Drukier, K. Freese, and D. N. Spergel, *Detecting Cold Dark Matter Candidates*, *Phys. Rev.* **D33** (1986) 3495–3508.
- [10] K. Freese, J. A. Frieman, and A. Gould, *Signal Modulation in Cold Dark Matter Detection*, *Phys. Rev.* **D37** (1988) 3388–3405.
- [11] J. Herrero-Garcia, *Halo-independent tests of dark matter annual modulation signals*, *JCAP* **1509** (2015), no. 09 012, [[arXiv:1506.03503](#)].
- [12] J. Herrero-Garcia, T. Schwetz, and J. Zupan, *On the annual modulation signal in dark matter direct detection*, *JCAP* **1203** (2012) 005, [[arXiv:1112.1627](#)].
- [13] J. Herrero-Garcia, T. Schwetz, and J. Zupan, *Astrophysics independent bounds on the annual modulation of dark matter signals*, *Phys. Rev. Lett.* **109** (2012) 141301, [[arXiv:1205.0134](#)].
- [14] N. Bozorgnia, J. Herrero-Garcia, T. Schwetz, and J. Zupan, *Halo-independent methods for inelastic dark matter scattering*, *JCAP* **1307** (2013) 049, [[arXiv:1305.3575](#)].
- [15] R. Bernabei et al., *Final model independent result of DAMA/LIBRA-phase1*, *Eur. Phys. J.* **C73** (2013) 2648, [[arXiv:1308.5109](#)].